Science Signaling
AAAS

www.sciencesignaling.org/cgi/content/full/10/477/eaai8133/DC1

Supplementary Materials for

Hyperactive locomotion in a *Drosophila* model is a functional readout for the synaptic abnormalities underlying fragile X syndrome

Risa Kashima, Patrick L. Redmond, Prajakta Ghatpande, Sougata Roy, Thomas B. Kornberg, Thomas Hanke, Stefan Knapp, Giorgio Lagna, Akiko Hata*

*Corresponding author. Email: akiko.hata@ucsf.edu

Published 2 May 2017, *Sci. Signal.* **10**, eaai8133 (2017)
DOI: 10.1126/scisignal.aai8133

This PDF file includes:

Text S1. LarvaTrack algorithm.

The objective of an object-tracking algorithm is to observe the path a target object takes over time through the static image frames of a video. The path is constructed of segments by inferring the movement of the target object between successive frames of video. If the target object is identified at position (1, 2) in frame N, and it is again identified at position (2, 1.5) in the successive frame N+1, the algorithm can infer that the target object moved from position (1, 2) to position (2, 1.5) along vector <1, -0.5> between those frames. Through the association of the target object location over many frames, a path can be observed.

An object-tracking algorithm for multiple objects must match multiple objects in frame N to the corresponding objects in frame N+1. A multiple object matching algorithm may apply heuristics such as distance and direction to improve matches, and in the presence of noisy object identification it may elect to exclude objects from the matching altogether. Objects identified in frame N which are excluded from matching are regarded as having not been identified in frame N+1, and are searched for again in frame N+2. Objects identified in frame N+1 which are excluded from matching are regarded as the origin of new paths.

We constructed a deterministic point tracker using the following tools and algorithms: To track and measure larva movement, the Python 2.7.10 language was used with the libraries OpenCV 2.4.12 and NumPy 1.10.1. To measure the scale of the video by identifying the petri dish and the coin, cv2.HoughCircles was used (*56*). To identify larvae in each frame, cv2.SimpleBlobDetector (http://docs.opencv.org/2.4/modules/features2d/doc/common_interfaces_of_feature_detectors.html#simpleblobdetector) was used. To guess the movement of the identified larva, we used cv2.calcOpticalFlowPyrLK (http://docs.opencv.org/2.4/modules/video/doc/motion_analysis_and_object_tracking.html#calcopticalflowpyrlk). To infer continuity between larvae identified in successive frames as described above, a variation of the Gale-Shapley stable matches algorithm (http://www.jstor.org/stable/2312726) was developed wherein “universities” are existing larva paths, “applicants” are detected blobs which haven’t been assigned to existing larva paths, and ‘preferences’ are rank-order by distance.

The LarvaTrack algorithm proceeded as follows: Input was represented as a zero-indexed array of images (FRAMES). The algorithm maintained the following state in three zero-indexed 2-dimensional arrays of (x, y) points (BLOBS, FLOW, and PATHS) wherein the major index indicates the frame, and the minor index indicates the path. The initialization step set PATHS[0] to the result of blob detection on the first frame of the video FRAME[0]. The algorithm advanced by inferring continuity between the paths seen through FRAME[f] and the points detected at FRAME [f+1]. The repeated step was as follows. Optical flow was run on FRAME[f], FRAME[f+1], and PATHS[f] to predict points to which paths moved, FLOW[f+1]. Blob detection was run on FRAME[f+1] to produce anchoring points, BLOBS[f+1]. A variation of stable matches was used to assign some

flow points from FLOW[f+1] to some anchoring points in BLOBS[f+1], as described above. Each of PATHS[f] received a new point in PATHS[f+1] at the corresponding index, as follows: Assigned flow points promoted from BLOBS[f+1] and unassigned flow points promoted from FLOW[f+1]. New indices were appended to PATHS[f+1] for each unassigned anchoring point from BLOBS[f+1] (fig. S4).

Text S2. Synthesis of TH263.

Synthesis of 4-(benzylsulfamoyl)benzoic acid: Benzylamine (2.42 g; 22.66 mmol; 10 equiv) was dissolved in 25 mL THF. 4-(chlorosulfonyl)benzoic acid (0.5 g; 2.27 mmol: 1 equiv) was added in portions and the reaction stirred at room temperature overnight. The reaction was diluted with 100 mL ethyl acetate and the organic layer was washed with 1N HCl (3* 50 mL) and dried over MgSO4. The solvent was removed under reduced pressure and the residue was recrystallized from MeOH/H_2O to afford 4-(benzylsulfamoyl)benzoic acid as a white solid. Yield: 0.55 g (83%). ^{1}H NMR (500 MHz, DMSO) δ 13.43 (s, 1H), 8.35 (t, *J* = 6.3 Hz, 1H), 8.08 (d, *J* = 8.6 Hz, 2H), 7.89 (d, *J* = 8.6 Hz, 2H), 7.28 – 7.25 (m, 2H), 7.24 – 7.19 (m, 3H), 4.02 (d, *J* = 6.3 Hz, 2H). ^{13}C NMR (126 MHz, DMSO) δ 166.27, 144.49, 137.42, 134.01, 130.08, 128.25, 127.61, 127.21, 126.77, 46.13. MS (ESI+): m/e = 292.08 $[M+H]^+$.

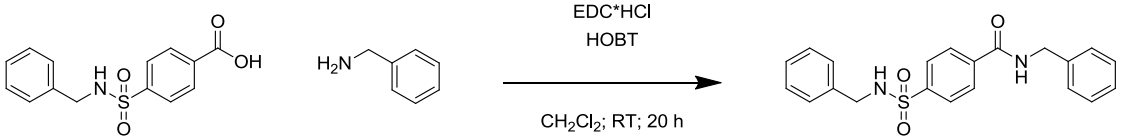

Synthesis of *N*-benzyl-4-(benzylsulfamoyl)benzamide: 4-(benzylsulfamoyl)benzoic acid (0.11 g; 0.39 mmol; 1 equiv), EDC*HCl (0.07 g; 0.47 mmol; 1.2 equiv) and HOBT (0.05 g; 0.39 mmol; 1 equiv) was dissolved in 10 mL DCM and stirred at room temperature. After 1 h benzylamine (0.06 g; 0.59 mmol; 1.5 equiv) was added and stirred for 20 h at room temperature. The reaction was quenched by the addition of 40 mL H_2O and the product extracted with ethyl acetate (50 mL). The organic layer was washed with 1N HCl (50 mL), brine (50 mL) and dried over $MgSO_4$. The solvent was removed under reduced pressure and the residue was recrystallized from *n*-hexane/ethyl acetate to afford *N*-benzyl-4-(benzylsulfamoyl)benzamide as a white solid. Yield: 0.08 g (55%). ^{1}H NMR (500 MHz, DMSO) δ 9.25 (t, *J* = 6.0 Hz, 1H), 8.28 (s, 1H), 8.04 (d, *J* = 8.5 Hz, 2H), 7.88 (d, *J* = 8.5 Hz, 2H), 7.37 – 7.31 (m, 4H), 7.30 – 7.19 (m, 6H), 4.50 (d, *J* = 6.0 Hz, 2H), 4.00 (s, 2H). ^{13}C NMR (126 MHz, DMSO) δ 165.10, 142.99, 139.34, 137.62, 137.50, 128.35, 128.27, 128.13, 127.60, 127.27, 127.21, 126.87, 126.57, 46.13, 42.76. MS (ESI+): m/e = 381.07 $[M+H]^+$.

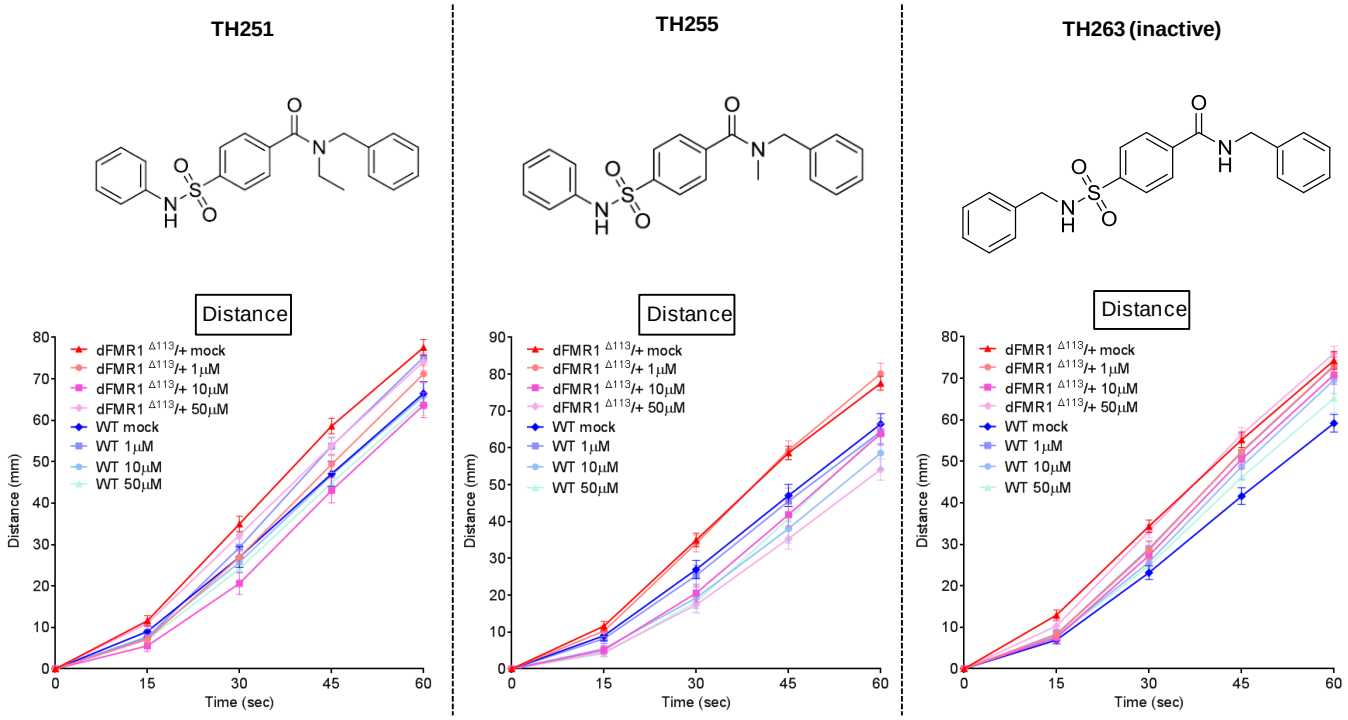

Fig. S1. Allosteric antagonists of LIMK1/2 reverse the locomotion phenotype in *dFMR1*$^{\Delta 113/+}$ larvae. *dFMR1*$^{\Delta 113}$/+ or wild-type (WT) third instar larvae were treated with 1, 10 or 50 μM LIMK1/2 antagonists (TH251 and TH255) or inactive analog TH263 (negative control) and subjected to the crawling assay for 1 min. Ten larvae were analyzed simultaneously. The assay was repeated 4 times. The average travel distance was quantitated by LarvaTrack. Data are means ± SEM. The chemical structures of the three compounds are shown above its respective assay data.

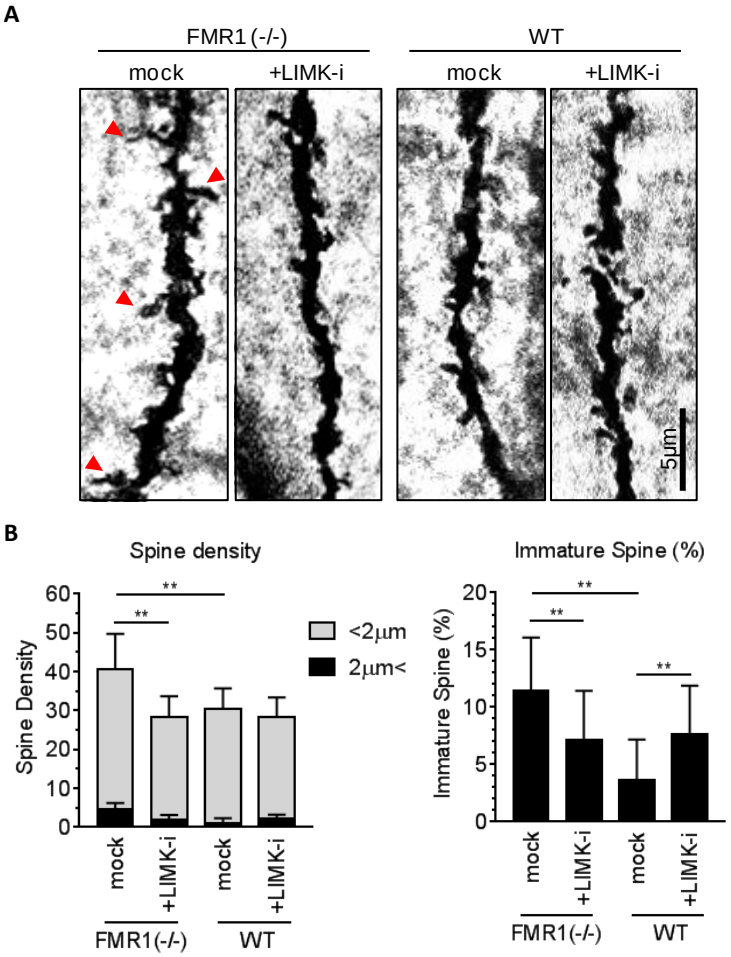

Fig. S2. Administration of LIMK-i ameliorates neuromorphological abnormalities in a mouse model of FXS. (**A**) *FMR1*-KO or wild-type (WT) littermate mice were treated with LIMKi-3 (LIMK-i) or DMSO (mock) by intracerebroventicular injection at P1 and P4, and the brains were isolated at P7, followed by Golgi staining. Representative images of dendritic spines of CA3 neurons are shown in high magnification. Abnormal dendritic spines are indicated by red arrows. Scale bar indicates 5 μm (*left*). (**B**) Dendritic spines in CA3 neurons were classified into two groups, short spines (<2 μm) or long immature spines (>2 μm), and counted. The total number of spines in 30 μm is shown as "spine density" (*left*) and the percentage of long immature spines (>2 μm) indicated by red arrowheads is calculated (*right*). More than seven independent CA3 neurons from three mice were analyzed. Means and SDs are indicated. ** P<0.01, by ANOVA with post hoc Tukey's test.

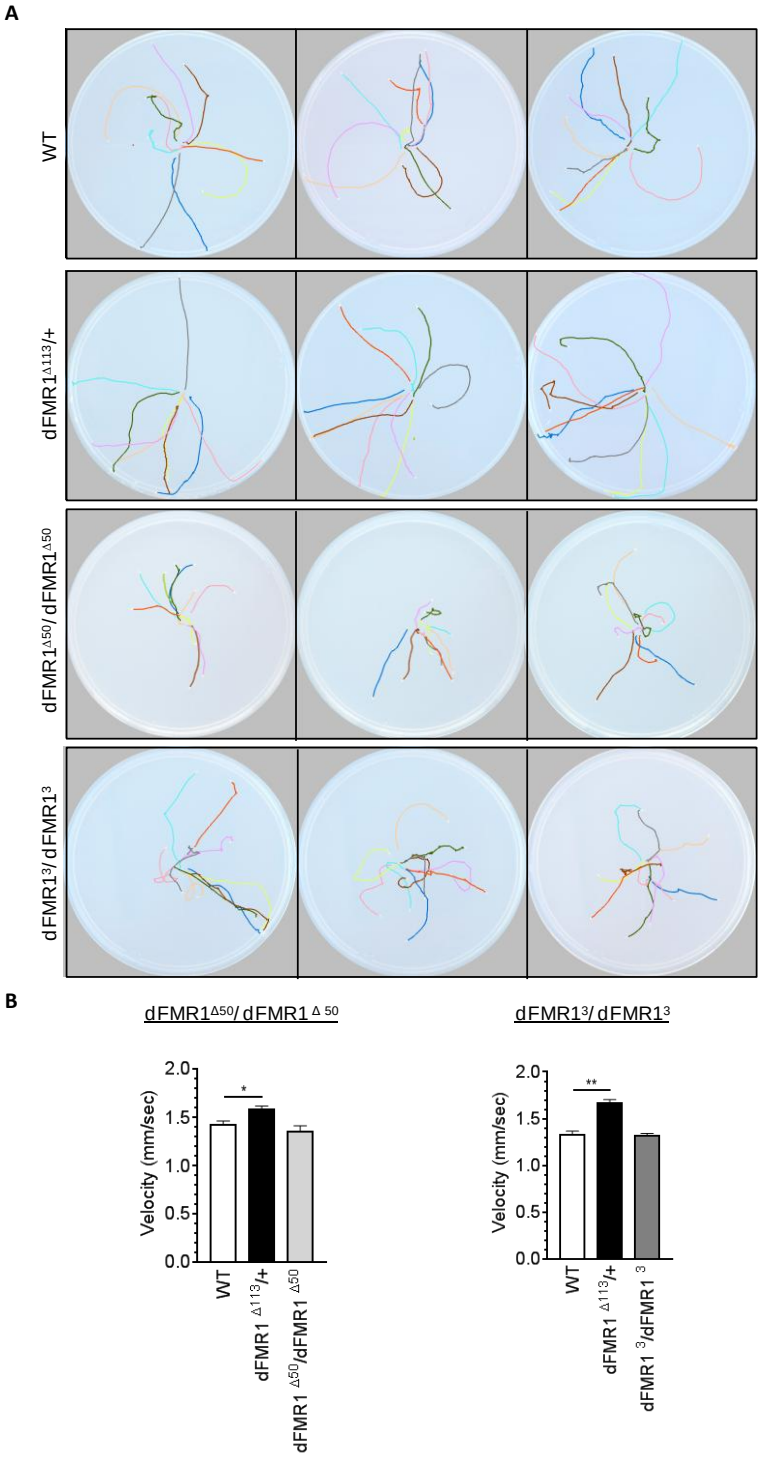

Fig. S3. Homozygous *dFMR1*$^{\Delta 50}$ and *dFMR1*^{3} mutants exhibit a frequently turning phenotype. (**A**) Representative path analysis data of wild-type (WT), *dFMR1*$^{\Delta 113}$/+, *dFMR1*$^{\Delta 50}$/ *dFMR1*$^{\Delta 50}$, and *dFMR1*^{3}/ *dFMR1*^{3} larvae crawling assay. The locomotion of WT larvae was traced individually and shown as lines. (**B**) The velocity was calculated. Means ± SEMs are plotted. **P*<0.05 , ***P*<0.01, by ANOVA with post hoc Dunnett's test.

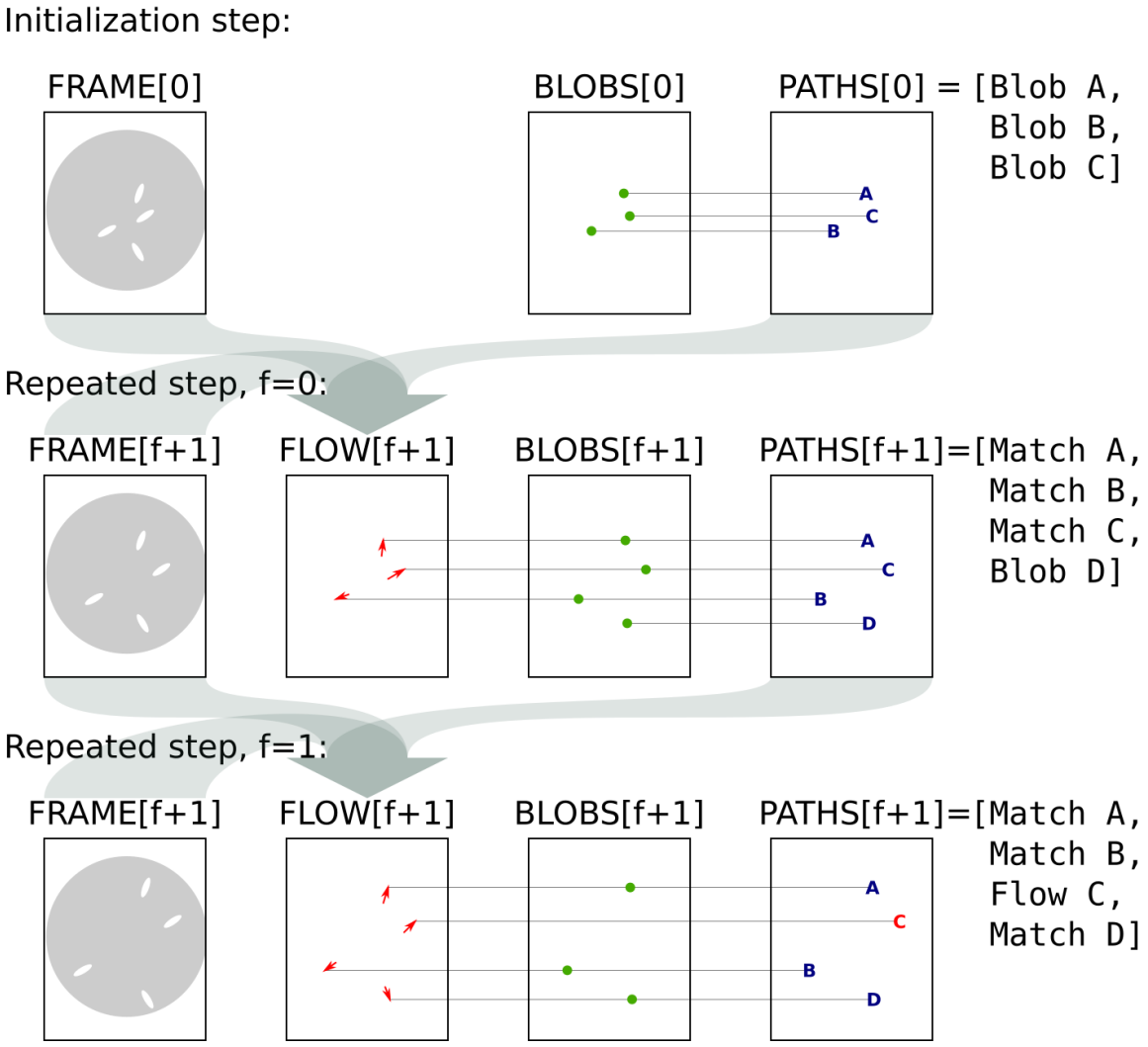

Fig. S4. The object tracker initialization and procedure at $f = 0$ and $f = 1$. At initialization, blob detection fails to find a fourth larva, but that larva is added the first time it is detected at f=0. At f=1, blob detection fails to find a larva that already has a path, and the unmatched flow point is promoted directly to the path result.